An integrated simulation approach for the design and analysis of complex mechatronic systems

Sikandar Moten, Goele Pipeleers, Jan Swevers, Wim Desmet
PMA Division, Department of Mechanical Engineering, KU Leuven, 3001 Leuven, Belgium
email: sikandar.moten@mech.kuleuven.be, goele.pipeleers@mech.kuleuven.be, jan.swevers@mech.kuleuven.be, wim.desmet@mech.kuleuven.be

ABSTRACT: Nowadays, virtual prototyping is often incorporated in the design process to accelerate the development of complex mechatronic systems. This implies that the use of experimental campaigns has to be reduced and the manufacturer has to rely more on simulation tools. This paper presents the on-going activities on the integrated simulation approach for the design and analysis of complex mechatronic system. This includes the development of a flexible multi-body model, a lumped parameter driveline model and a control system. In order to demonstrate the potential of the virtual design and analysis process for modern mechatronic systems, an industrial machine tool is used as a case study. It is observed that the dynamic characteristics of the machine are dependent on the spatial position of the head. However, it is found that these configuration dependent dynamics have negligible influence on the planar motion of the machine. In order to predict the dynamic behavior of the machine, forecast the influence of specific design changes, and assess the impact of different control architectures with full confidence, the model needs to be validated. To this end, the simulations of the model are compared with the results obtained on a physical prototype.

KEY WORDS: Mechatronic system modeling; Virtual prototyping.

1 INTRODUCTION

The rising demands of high speed and high precision mechatronic systems, while reducing the time to market, motivates to include virtual prototyping in the design and development process, see [1], [2], [3] and [4]. Examples of such mechatronic systems include pick-and-place machines [5], milling machines [4], water jet cutting machines [3], weaving looms [6], 3D rapid prototyping machines, cartesian mechanisms etc. Such systems consist of several sub-systems or modules from different engineering disciplines varying from hydraulic components over controller hard- and software till electro-mechanical drivelines and storage elements.

In this paper, an integrated approach is presented for the modeling of mechatronic system. In this approach, each module is described separately in their most suitable formalism. The formalism in which these different laws are described depends on the complexity of the system and the desired accuracy; for the machines having elastic components and subjected to significant excitations, flexible multi-body models are required [7]. In contrast, an electric motor or a gear-box can, in most cases, be described by ideal lumped components. These modules or sub-systems are combined with each other via a bondgraph approach. A more detailed description is given in [6] and [8]. After building the plant model, a controller can be concatenated with the model of the physical system.

The coupling of such sub-systems allows us to test different control strategies [5], to evaluate the performance and robustness of the closed loop system [9], to analyze the impact of specific design changes and to assess the performance of reduced order models as well as reduced order controllers. Moreover, if a prototype of the system is available, this methodology allows to use simulation results to prepare experiments. The obtained experimental results can then be used to update the model. A 3-axes machine tool is used to demonstrate the approach in this paper.

1.1 System description

The industrial case study is a 3-axes machine tool, shown in Figure 1. The gantry of the machine tool moves in the X-direction, whereas the head is capable of moving along the Y and Z directions. As the variation in the Z-axis is expected to be small during machine operation and has a negligible influence on the machine performance, it is not taken into account for the analysis. The total mass of the gantry is 330 kg including the head mass of 50kg. The machine is equipped with two rotary motors, along the sides of the gantry, which drive the machine in X-direction via rack and pinion mechanisms. In addition, a linear motor is used to actuate the machine head in Y-direction. The displacement of the rotary motors are measured via built-in encoders, whereas, the position of the linear motor is measured by an optical encoder attached along the length of the gantry. Moreover, Bernecker and Rainer (B&R) Automation studio platform is used to implement controllers for the physical prototype. The purpose of this machine is to move the tool center point (TCP), fixed on the machine head, along a given trajectory in the workspace as fast and precisely as possible. An experimental prototype of the machine tool is shown in Figure 2.

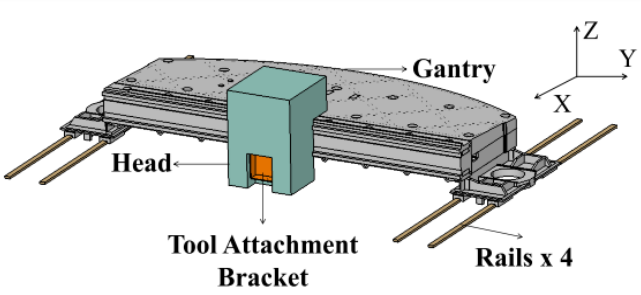

Figure 1. CAD model of an industrial machine tool

Figure 2. Prototype of an industrial machine tool

1.2 Paper Outline

This paper presents an integrated approach for the mechatronic modeling of an industrial machine tool. To this end, Section 2 describes the mechatronic system modeling in detail. Section 3 describes the machine tool prototype used to validate the obtained model, discusses the performed experiments and measurement setup. Section 4 discusses the influence of configuration dependent dynamics with respect to the spatial position of the machine head. Section 5 compares simulation results and experimental data, and Section 6 concludes this paper.

2 MECHATRONIC SYSTEM MODELLING

The complete mechatronic model combines a 3D model flexible multi-body (FMB) model of the structure, a 1D lumped parameter model of the driveline and a controller. This Section describes these different sub-systems and discusses how to combine them in an integrated architecture.

2.1 3D Flexible Multi-body model

The FMB model requires models of flexible and rigid bodies, and mechanisms for the interconnecting rigid and flexible bodies. In addition, a connection with the rest of the system (i.e. 1D model and controller) needs to be established. Moreover, a reduced order model is required for efficient simulation purposes. In the sequel, these elements are described.

- Rigid and flexible bodies:

For the current case study, it is assumed that the head of the machine tool is a rigid body. The gantry and the tool attachment bracket, shown in Figure 1, will undergo elastic deformation during machine operation in addition to the rigid body motion.

Thus, the FMB model of the machine tool consists of a rigid head, a flexible tool attachment bracket fixture and a flexible gantry. Building a flexible body/assembly starts with creating the finite element (FE) meshes of the individual parts of the assembly. As a FE mesh is based on the actual geometry, a computer aided design (CAD) model is used as a starting point for creating the mesh. In order to develop the physical prototype, shown in Figure 2, the designers usually develop a detailed CAD model of the machine tool with all the components and auxiliary systems. In practice, not every detail of the geometry is required or taken into account. Small auxiliary systems are neglected or assumed rigid to decrease the complexity and the degrees of freedom (DOF) in the FE mesh. Other details like fillets, chamfers, small holes, grooves etc. are removed if they have a negligible effect on the mode shapes and eigenfrequencies of the individual body[10]. The next step is to combine the different FE meshes of the components together to form an assembly.

The flexible model of the tool attachment bracket consists of an aluminum bracket together with the lumped mass of the tool. The FE model of this attachment bracket has approximately 32000 DOF. The complete gantry has 5 components that are connected to each other via bolted connections. Three of these are made up of aluminum and the other two are made up of steel. Each bolted connection is represented by a multiple point constraint (RBE2 element). The auxiliary systems (i.e. motors, cables, bellows, valves etc.) are added to the FE model as an equivalent point mass with the same inertial properties. Similar multiple point constraints (RBE3 element) are used to attach them to the FE mesh. The connection between the gantry and the guides are defined by a 6-DOF stiffness relation (CELAS element), where the stiffness is set to zero in the translational direction. The complete gantry model has approximately 0.7 million DOF. The FE models, shown in Figure 3, have been meshed sufficiently dense to ensure convergence.

Figure 3. FE models of the flexible bodies [Models are scaled]

The model parameters are not always known beforehand, are uncertain or vary over time. This makes it very difficult to correlate the model with reality as the number of uncertain parameters is substantial and thus creating a vast space of possible parameter combinations. The connection between the gantry and the guides are defined by the stiffness values in 5 directions (1 translational direction is left free). A limited set of sensitivity analyses have been performed for different values of stiffness in the guides, and from that it can be conclude that the dynamic behavior is highly dependent on these flexibilities. For the current simulation model, the

stiffness values recommended by the machine tool manufacturer are used. These values correspond to one-fourth of the stiffness values given in the datasheet of the guides. The actual values for the stiffness are still uncertain and depend on preload, manufacturing tolerances, lubrication, assembly alignments, etc.

In order to understand the dynamic characteristics of the flexible components, the numerical modal analyses have been performed for: (i) the tool attachment bracket with clamped boundary condition and (ii) the gantry with the head in the middle and the left extreme positions. In the latter case, the head is added as a point mass. Figure 4 and Figure 5 illustrate the first bending mode of the tool attachment bracket and the gantry machine, respectively. It can be seen that the mode shape and the eigen-frequency of the gantry machine are dependent on the spatial position of the head. Based on the visual analysis of this bending mode, it is expected that the planar motion performance of the machine (X-Y displacement) will be influenced negligibly by this mode. In contrast, it is expected that the first bending mode of the tool attachment bracket will influence the planar motion of the machine significantly.

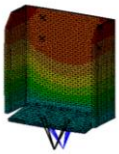

Figure 4. Mode shape for the first bending mode of tool attachment bracket (182 Hz)

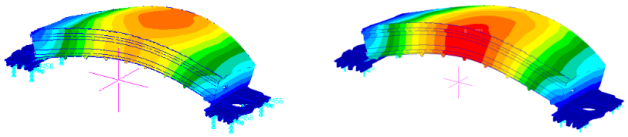

Head at the left position (116 Hz)

Head at the middle position (102 Hz)

Figure 5. Mode shape for the first bending mode of gantry

It is clear from the FE analysis that the dynamic behavior of the gantry machine is configuration dependent. In order to determine to which extend this dependency influences the machine planar performance, we need to identify the system behavior with respect to system inputs. Therefore, we will continue with developing the FMB model.

- Mechanism:

Next, a mechanism can be built by defining joints and constraints between the different bodies at the interface points. All joints are assumed to be ideal and have no flexibilities nor friction. Translational joints are used between guides and rails, and a flex-point curve joint (i.e. joint between flexible and rigid bodies) is used to attach the rigid head with the flexible gantry. The flexibilities in the guides for the X-axis are already incorporated in the FE model, whereas the guides for the Y-axis are assumed to be rigid. Moreover, it is assumed that the rails for the X-axis guides are rigid and attached rigidly with the ground.

- Interface:

When the flexible multi-body model is created, an interface with the rest of the system (i.e. 1D model) is established via control nodes. These control nodes can be used to apply forces and measure displacement, velocity and acceleration. The flexible multi-body model is developed in LMS Virtual.Lab Motion Environment [11], and is shown in Figure 6.

- Model reduction:

The developed FE models for the gantry and the tool attachment bracket have approximately 0.7 million and 32000 DOF, respectively. These models are not directly suitable for efficient computer simulation purposes. Therefore, there is a need to obtain reduced order models. The reduced order models are computed by using the component mode synthesis (CMS) technique [12] - a well-known method in linear structural dynamics. Craig-Brampton modes are computed for the gantry (without head) and the tool attachment bracket in a solver package i.e. MSC/MD NASTRAN. With this method, each mode of the flexible body adds one generalized coordinate to the system [11].

The interface or connecting DOFs are preserved [13]. The total number of modes used for the simulation of the gantry and tool attachment bracket are equal to 60 and 38, respectively. The obtained reduced order models via CMS are suitable for simulation purposes. Finally, it is necessary to mention that 2.5% modal damping is added. This estimate is based on the experimental modal analysis performed earlier on the physical prototype.

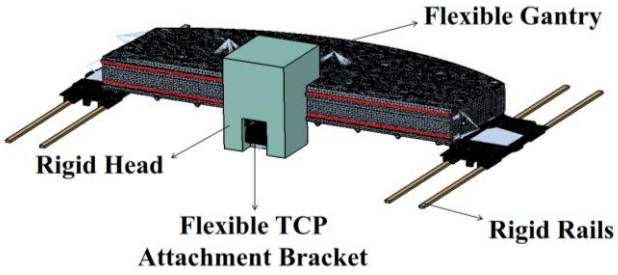

Figure 6. Flexible multi-body model (LMS Virtual.Lab Motion Environment)

2.2 1D Multi-physics model

The other relevant parts of the system, that do not require a detailed description of the geometry, are modeled by a lumped parameter approach using the bondgraph method. Although only mechanical components are described for this particular exercise, this is not a constraint for the methodology. The bondgraph method couples components together by means of energy relations which are independent of their physical domain. This means that every interface point consist of effort and flow variables that uniquely define the power at that particular interface point [6]and [8]. This approach of energy relations can be exploited to integrate sub-systems with different formalism together i.e. lumped parameter models can

be combined with flexible multi-body models as long as an appropriate energy relationship is defined at the interface points. LMS Imagine.Lab AMESim provides a platform for modeling and analysis of physical multi-domain systems, governed by ordinary differential equation ODE or differential algebraic equations DAE [14].

This platform is used to model the lumped parameter driveline model. The modeled driveline for the X-axis consists of a motor inertia, a gear-box (modeled as an ideal reducer), a rack and pinion mechanism (modeled as an ideal transformer), and the lumped stiffness and damping in the driveline. The modeled drive-line for the Y-axis consists of a linear force input. The stiffness and damping values of the X-driveline is provided by the machine manufacturer. All the other parameters are taken from the datasheets of the components. The models developed in AMESim for both the axes are shown in Figure 7.

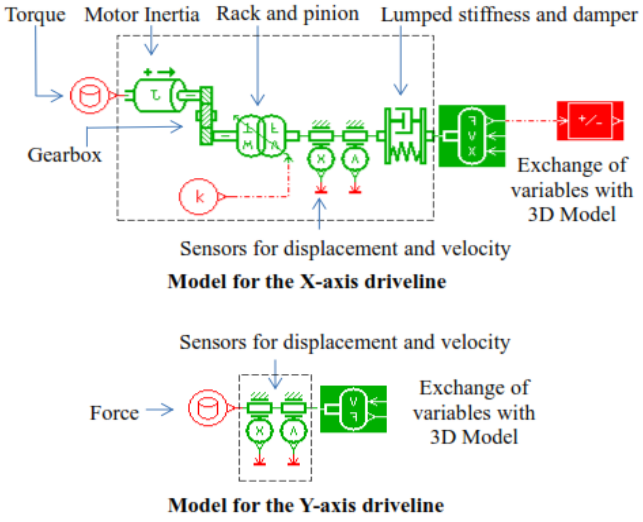

Figure 7. One-dimensional lumped parameter driveline models for the X and Y axes (LMS Imagine.Lab Environment)

2.3 *Controller*

The accuracy of the machine operation is significantly dependent on the performance of the servo drive's controller. The purpose of the machine is to follow desired geometric trajectories as quickly and precisely as possible. This implies that the machine should follow geometric trajectories time optimally with limits on the deviation of TCP from the given trajectories. In machine industry, this deviation is referred to as contouring error i.e. the component of error perpendicular to the given trajectory [15]. A cascaded scheme with the P (proportional) and PI (proportional-integral) controllers for the position and velocity loops, respectively, together with velocity and acceleration feedforward has been chosen, as shown in Figure 8. More on servo drive control for machine tools can be found in [15]. There are two main reasons for choosing this type of control scheme: (i) this cascaded control is very common in machine industry, (ii) at present, this scheme is implemented on the B&R Automation studio platform for the physical prototype. In order to compare the closed-loop performance of the real machine and virtual model, the controller parameters tuned on the physical prototype are used for the virtual model. The controllers for the X and Y axes drives are attached to the corresponding 1D drive-line models in AMESim.

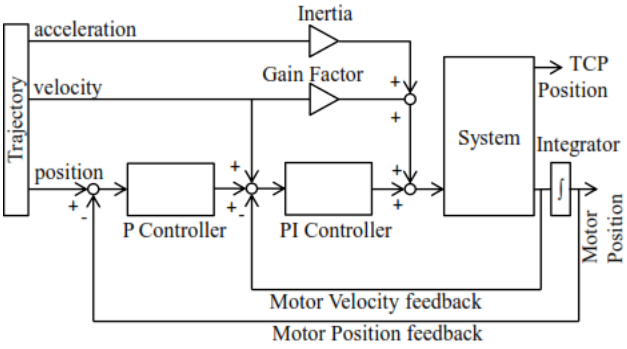

Figure 8. Schematic of cascaded controller

2.4 *Model Integration*

The 1D lumped parameter model and the 3D FMB model are built separately on different platforms. In order to analyze the overall dynamic behavior of the system, these models have to be simulated in an integrated fashion. To accomplish this, the following two approaches are supported by Imagine.Lab AMESim and Virtual.Lab Motion platforms:

- Co-simulation: With co-simulation, the state equations of the different sub-systems (1D/3D) are solved independently and their data is exchanged at discrete time steps.
- Coupled simulation: In this case, the complete set of state equations of all the sub-systems is processed with a master solver.

In each case, the different sub-systems have to be treated as an equivalent bondgraph component in order to interface them with each other. In this particular case, the most straightforward option is to combine both sub-systems via co-simulation. This approach is justified as long the communication interval between the two platforms is small enough in order to ensure that fast dynamics are not missed by the solver. A communication interval of 100 µs has been chosen for the simulation; however, the data is sampled every 400 µs to remain consistent with the experimental measurement setup.

3 EXPERIMENTAL AND VIRTUAL IDENTIFICATION

Now, the developed mechatronic model is ready for the analysis via co-simulation. This implies that the dynamic behavior of the system can be identified and validated. Since, a physical prototype of the machine tool is available, the same experiments can be performed on the physical and virtual prototype. The obtained results can be compared to check the accuracy of the model. In this Section, first, the experimental measurement setup is discussed. Next, the technique used to identify the dynamic behavior of the physical and virtual machine is described. Finally, the obtained results are presented and compared.

3.1 *Experimental Setup*

The motors displacements are recorded by synchronously logging the motor encoder signals. A Heidenhain KGM grid encoder [16] is used to measure the response at the TCP. The KGM sensor system comprises a scanning head and a grid plate embedded on a base plate. The advantage of this measurement system is that it allows us to perform contactless displacement measurement of the TCP. In order to perform these measurements, the base plate is mounted on the table of the machine tool and aligned by using a dial indicator. Then, the scanning head is attached to the machine head by using a sheet metal bracket fixture.

3.2 *System Identification*

Since it is not safe to perform open loop identification experiments on the actual physical prototype, closed loop frequency domain identification performed to identify the machine tool, see [17]. The same technique is used to identify the model of the virtual machine tool with virtual sensors. Periodic multi-sine (with frequency components between 10 and 500 Hz) excitation experiments are performed in order to estimate frequency response functions (FRFs). These excitation signals are injected as an input current to the motors. The current signals are converted to force and torque (correspond to the linear and rotary motors, respectively), for the virtual prototype. During these experiments, the position controller is not used, whereas the velocity controller is detuned. The reference velocity is set to zero. The FRFs from X-axis motor torque to the displacements of the rotary motor and TCP in X-direction are shown in Figure 9 and Figure 10, respectively. In addition, the FRFs from Y-axis force to the displacements of the linear motor and TCP in Y direction are shown in Figure 11 and Figure 12, respectively.

3.3 *Results*

The following observations are made:

- X-axis: The small differences in phase at low frequencies observed both in the motor encoder and TCP FRF's indicate the existence of friction in the X-axis driveline. The magnitude and phase of the encoder FRF correspond very well up to a certain level of accuracy. However, the TCP FRF shows significant discrepancies at the frequencies higher than 125 Hz. The flexible mode near 185 Hz also correlates with the simulation. The mismatches for the frequencies higher than 125 Hz are due to the un-modeled dynamics or uncertain parameters. This is currently under investigation.
- Y-axis: Similar to the X-axis, the small differences in phase at low frequencies observed both in the motor encoder and TCP FRF's indicate the existence of friction in the Y-axis driveline. The mass line behavior for these FRFs matches very well with the simulation model for the frequencies up to 100 Hz. For the encoder FRF, the small discrepancies at higher frequencies (such as at 150 Hz) are due to the joint stiffnesses between different components inside the head. For the TCP FRF, the discrepancies at higher frequencies, both in magnitude and phase, are due to the un-modeled dynamics.

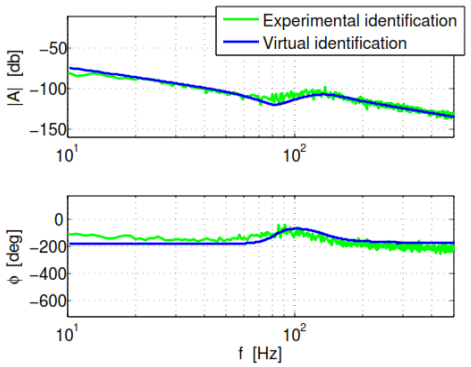

Figure 9. FRF from X motor torque to X motor encoder

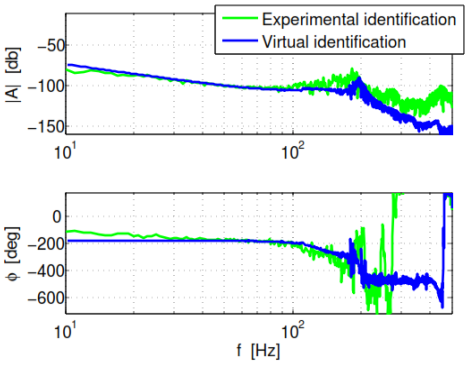

Figure 10. FRF from X motor torque to TCP displacement in X direction

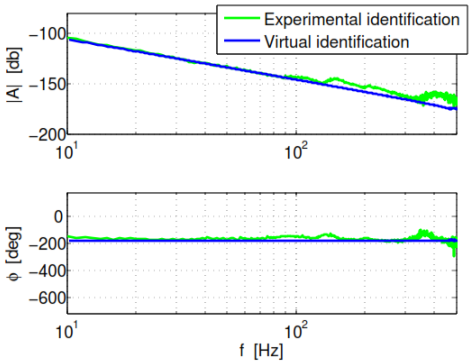

Figure 11. FRF from Y motor force to Y motor encoder

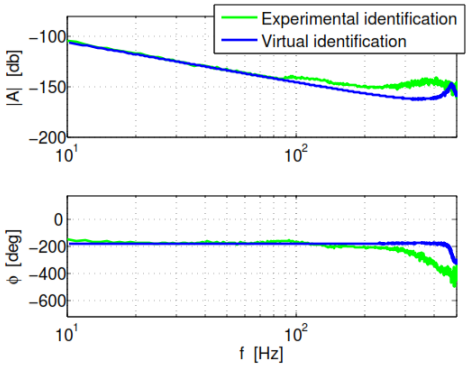

Figure 12. FRF from Y motor force to TCP displacement in Y direction

3.4 Discussion

The comparison of the FRF's identified on the experimental and virtual prototypes reveals a good correspondence between model and real system and a number of discrepancies. There are a number of possible reasons for these discrepancies: (i) uncertain parameters (such as stiffness in the guides, damping in the system, material properties), (ii) modeling assumptions and simplifications (for instance, neglected friction and flexibilities in the joints), (iii) manufacturing tolerances, (iv) un-modeled dynamics(for instance, rigid head assumption), (v) environmental and other boundary conditions.

However, more experimental investigation is required to further improve the model. Consequently, this will facilitate to tune and update the model further.

4 INFLUENCE OF CONFIGURATION DEPENDENT DYNAMICS

In section 2.1, the FE analyses have shown that the dynamic characteristics (bending mode) of the machine are dependent on the spatial position of the head. However, both in the virtually and experimentally identified system, the bending mode is not observable at TCP in X and Y direction, see Figure 10 and Figure 12. In the sequel, the influence of configuration dependent dynamics is investigated.

The periodic multi-sine excitation experiments are repeated on the prototype for two different spatial positions of the head i.e. middle and left extreme. The Heidenhain KGM grid encoder is capable to log planar motion data i.e. X and Y displacement in our case. In order to measure the TCP displacement in Z-direction, additional PCB ICP accelerometers are used. For the data acquisition of these additional accelerometers, LMS SCADAIII hardware in combination with LMS Test.Lab software are used.

The FRF from X-axis motor torque to the TCP displacement in X-direction is shown in Figure 13. It can be seen that the configuration dependent bending mode is not observable for both spatial positions of the head. The flexible mode near 185 Hz correlates well with the mechatronic model. This mode corresponds to the bending mode of the tool attachment bracket, see Figure 4.

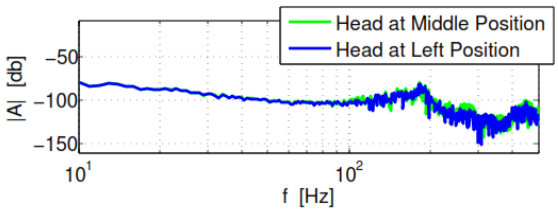

Figure 13. FRF from X motor torque to TCP displacement in X direction for different spatial position of the head

The FRF from Y-axis force to TCP the displacement in Y direction is shown in Figure 14. It can be seen that the configuration dependent bending mode is not observable.

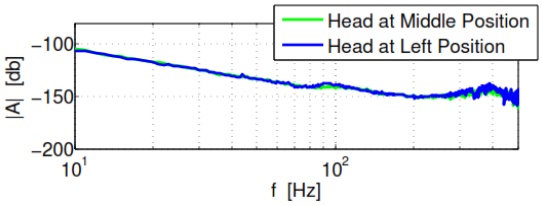

Figure 14. FRF from Y motor force to TCP displacement in Y direction

In order to observe the configuration dependent bending mode, the FRF from X-axis motor torque to the TCP displacement in Z-direction is shown in Figure 15. This figure clearly shows that the resonance peak around 100 Hz depends on spatial position of the head (i.e. 98 Hz and 112 Hz for middle and left head positions, respectively). This mode corresponds to the bending mode of the gantry machine, see Figure 5. However, the influence on the TCP displacement in Z direction doesn't degrade machine planar performance.

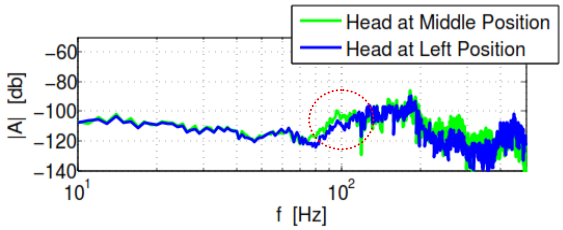

Figure 15. FRF from X motor torque to TCP displacement in Z direction

Based on the above analyses, it is concluded that the configuration dependent dynamics have negligible influence on the planar motion (X-Y displacement) of the machine TCP. This may be due to the fact that either this mode is not excited well with the motor inputs or the mode shape doesn't influence the TCP displacement in X and Y directions.

5 CLOSED-LOOP SYSTEM PERFORMANCE EVALUATION

Figure 16 shows the geometric tool path used to evaluate the system performance in closed-loop, both for the physical and virtual prototype. This trajectory is a 50 mm x 50 mm square with 5 mm filleted corners. Based on this geometric tool path, time-optimal motion trajectories for both axes are generated using the approach developed by Van Loock et al. [18] allowing a geometric error of 1 µm and constraints on axes velocity, acceleration and jerk equal to 0.5 m/s, 20 m/s^2 and 800 m/s^3, respectively. The computed positions, velocities and accelerations are used as inputs to the controller shown in Figure 8. The controller parameters for the physical and virtual prototype are identical.

Figure 17 compares the measured and simulated TCP displacements. It can be observed that the maximum absolute contouring error at the TCP is 48 µm and 30 µm for the physical and virtual prototype, respectively. The difference between the experimental and simulation results is due to the

mismatches between the experimentally identified and virtual models. However, for the manufacturers of machine tools, such a qualitative match between the actual and virtual machine at early design stages is very useful to assess design changes.

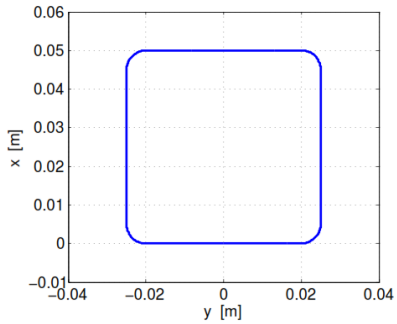

Figure 16. 50 mm x 50 mm square with 5 mm filleted corners

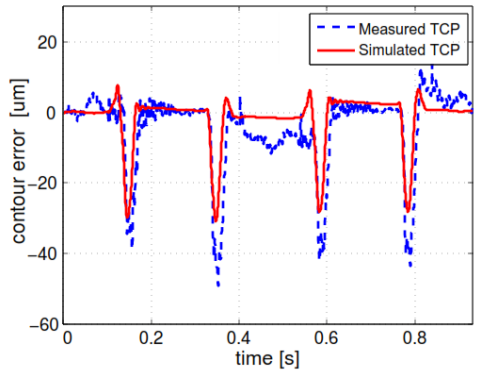

Figure 17. Comparison of measured and simulated TCP contouring error

6 CONCLUSION

This work presented the on-going research activities in development, simulation and validation of mechatronic models for complex mechatronic systems such as the considered machine tool. A flexible multi-body model and a 1D lumped parameter model together with the controller are developed. A co-simulation is set up between these models.

It is shown that unlike 1D lumped modeling approach, the flexible multi-body approach allows us to model the elastic deformation behavior of the system (i.e. gantry and tool attachment bracket). In addition, it is observed that the dynamic characteristics of the machine are dependent on the spatial position of the machine head. However, it is found that these configuration dependent dynamics have negligible influence on the planar motion of the machine. In order to correlate the virtual model with reality, the modeler has to use engineering intuition, assumptions and experience, experimental data and analysis to decide on various factors; for instance, which parts of the machine can be assumed rigid. Once the mechatronic model correlates well with the experiments, it is a very useful tool to predict the dynamic behavior of the machine at early design stages. The model can also be used to forecast the influence of specific design changes, and to assess the impact of different control architectures. This helps to reduce the time consuming and costly procedure of making physical prototypes after every design change. Consequently, the manufacturers of mechatronic system can reduce time to market while meeting with market demands.

ACKNOWLEDGMENTS

The research of S. Moten is funded by an Early Stage Researcher grant within the European Project IMESCON Marie Curie Initial Training Network (GA 264672). The IWT Flanders within the Dilacut project is also gratefully acknowledged for its support. Finally, this work also benefits from the KU Leuven Optimization in Engineering Center (OPTEC) and Belgian Programme on Interuniversity Attraction Poles, initiated by the Belgian Federal Science Policy Office (DYSCO). Goele Pipeleers is Postdoctoral Fellow of the Research Foundation Flanders (FWO).

REFERENCES

[1] A. Fortunato and A. Ascari, "The virtual design of machining centers for HSM: towards new integrated tools," *Mechatronics*, vol. 23/3, pp. 264–278, 2013.

[2] H. Van Brussel, P. Sas, I. Németh, P. D. Fonseca and P. V. Braembussche, "Towards a mechatronic compiler," *IEEE/ASME Transactions on Mechatronics*, vol. 6/1, pp. 90–105, 2001.

[3] A. Jönsson, J. Wall and G. Broman, "A virtual machine concept for real-time simulation of machine tool dynamics," *International Journal of Machine Tools and Manufacture*, vol. 45/7, pp. 795–801, 2005.

[4] G. Bianchi, F. Paolucci, P. van den Braembussche and H. van Brussel, "Towards virtual engineering in machine tool design," *CIRP Annals - Manufacturing Technology*, vol. 45/1, pp. 381–384, 1996.

[5] M. M. Da Silva, W. Desmet, H. Van Brussel, "Design of mechatronic system with configuration-dependent dynamics: Simulation and optimization," *IEEE/ASME Transactions on Mechatronics*, vol. 13/6, pp. 638–646, 2008.

[6] J. Croes, A. Reveillere, S. Iqbal, D. Coemelck, B. Pluymers and W. Desmet, "A combined 1D-3D simulation approach for the energy analysis of a high speed weaving machine," *In Proceeding of International Conference on Noise and Vibration Engineering, ISMA*, 2012.

[7] M. Zaeh and D. Siedl, "A new method for simulation aof machining performance by integrating finite element and multi-body simulation for machine tools," *CIRP Annals - Manufacturing Technology*, vol. 56/1, pp. 383–386, 2007.

[8] P. C. Breedveld, "Port-based modeling of mechatronic systems," *Mathematics and Computers in Simulation*, vol. 66/2-3, pp. 99–127, 2004.

[9] W. Symens, H. Van Brussel and J. Swevers, "Gain- scheduling control of machine tools with varying structural flexibilities," *CIRP Annals - Manufacturing Technology*, vol. 53/1, pp. 321–324, 2004.

[10] Y. Altintas, C. Brecher, M. Weck and S. Witt, "Virtual machine tool," *CIRP Annals-Manufacturing Technology*, vol. 54/2, pp. 115–138, 2005.

[11] LMS Virtual.Lab. *On-line help*, Rev10 SL-1, 2011.

[12] B. D. Kraker, *A Numerical-Experimental Approach in Structural Dynamics.* Shaker Publishing, Maastricht, 2013.

[13] M. M. D. Silva, *Computer-aided integrated design of mechatronic system*, Ph.D. dissertation, KU Leuven, 2009.

[14] LMS Imagine.Lab AMESim. *Integration algorithm used in AMESim*, Technical bulletin No. 102, 2012.

[15] Y. Koren, "Control of machine tools," *Journal of Manufacturing Science and Engineering*, vol. 119, pp. 749–755, 1997.

[16] Heidenhain. *Measuring devices: For machine tool inspection and acceptance testing*, [Online] Available from: <http://www.heidenhain.de> [Accessed 15 November 2013].

[17] R. Pintelon and J. Schoukens, *System Identification: A Frequency Domain Approach, Second Edition*. John Wiley & Sons, Inc., Hoboken, NJ, USA, 2012.

[18] W. Van Loock, S. Bellens, G. Pipeleers, J. De Schutter and J. Swevers, "Time-optimal parking and flying: Solving path following problems efficiently*," In Proceedings of the IEEE International Conference on Mechatronics (ICM). IEEE*, pp. 841–846, 2013.